

# Terahertz-Bandwidth Characteristics of Coplanar Transmission Lines on Low Permittivity Substrates

Heng-Ju Cheng, John F. Whitaker, *Member, IEEE*, Thomas M. Weller, and Linda P. B. Katehi, *Senior Member, IEEE*

**Abstract**—Coplanar striplines and waveguides capable of supporting ultra-high-frequency pulses over many millimeters of propagation length have been fabricated on low-permittivity substrates, including a durable 1.4- $\mu\text{m}$ -thick membrane. These transmission lines were characterized using broadband pulses from a novel *in situ* optoelectronic test-signal generator together with an electro-optic probe tip and an optically-based sampling technique. Pulse-propagation characteristics for the coplanar lines on the low-permittivity substrates have been compared in both the time and frequency domains with the transmission behavior of lines on GaAs substrates. A semi-empirical model has also been used to simulate the experimental results with good agreement, helping to indicate the origin of the distortion mechanisms involved. In addition, for the coplanar waveguide structures, waveforms corresponding to the even and odd modes have been individually resolved in the time domain for lines fabricated on the GaAs and membrane substrates.

## I. INTRODUCTION

WITH advances in the field of microelectronics, it is no longer unusual for electronic and optoelectronic devices with multihundred-gigahertz bandwidth to be designed and fabricated. For example, MSM photodiodes with sub-micron finger spacings can have a bandwidth in excess of 500 GHz [1], submicron HEMT devices can have a cut-off frequency over 300 GHz, and quarter-micron Schottky diode mixers are able to operate at 2.5 THz [2]. However, in order to effectively exploit the ultrafast response of these kinds of devices, wave-guiding structures having a bandwidth comparable to that of the high-speed devices must be devised. Unfortunately, traditional guiding structures such as microstrip, coplanar stripline, and coplanar waveguide, when fabricated on semiconductor substrates, can only support a limited signal bandwidth (approximately 150 GHz) without excessive dispersion and loss. The main reason for the enormous high-frequency signal distortion found in planar transmission lines is the permittivity mismatch between the substrate and the air. Because of this mismatch, guided waves on transmission lines radiate some of their energy into the substrate as a shock wave [3].

Manuscript received April 1, 1994; revised July 8, 1994. This work was supported in part by the National Science Foundation, the Center for Ultrafast Optical Science under grant STC PHY 8920108 and by the Office of Naval Research.

H. Cheng and J. F. Whitaker are with the Center for Ultrafast Optical Science, University of Michigan, Ann Arbor, MI 48109-2099 USA.

T. M. Weller and L. P. B. Katehi are with the NASA Center for Space Terahertz Technology, Department of Electrical Engineering and Computer Science, University of Michigan, Ann Arbor, MI 48109-2122 USA.

IEEE Log Number 9405412.

One way to avoid shock-wave radiation loss is to eliminate the inhomogeneous dielectric medium by capping the transmission line surface with a mechanical superstrate of similar permittivity [4]. This method can work well if there is essentially no air gap between the superstrate and the substrate, a condition that is very difficult to achieve. For a substrate which already supports devices and interconnection lines, where the surface topography is not flat, the only way to achieve the dielectric match is to deposit or regrow a superstrate with thickness approximately equal to the cross-sectional size of the transmission line. Since it is not practical to use chemical vapor deposition (CVD) to deposit, or molecular beam epitaxy (MBE) to regrow, several tens of micrometers of high-quality and low-loss superstrate material, a superior approach appears to be the reduction of the substrate permittivity. Reference [5] has demonstrated this kind of guiding structure (named the CAT line) where the substrate material has been mostly etched away, leaving free-standing metal coplanar electrodes with periodic support posts. Reference [6] also used a free-standing quantum-well thin film as the substrate for a transmission line where very low signal dispersion has been demonstrated.

In this paper, we investigate both experimentally and computationally the propagation of broadband subpicosecond electrical pulses on coplanar transmission lines fabricated on low-permittivity substrates and driven by a novel integrated *in situ* electrical pulse generator. Both a 1.4- $\mu\text{m}$ -thick composite dielectric membrane and UV-grade fused silica have been employed as substrates for coplanar stripline (CPS) and coplanar waveguide (CPW) structures. Because of the reduced mismatch in substrate/superstrate permittivity for these lines, superior propagation characteristics have been experimentally demonstrated in both time- and frequency-domains as compared to lines fabricated on GaAs. The propagation factor calculated from a semi-empirical lumped-element model has been compared with the values deduced from the experimental data with good agreement, helping to justify the applicability of the semi-empirical model to pulse propagation studies on coplanar lines printed on low-permittivity substrates. Furthermore, the inherently higher impedance realized for transmission lines on low permittivity substrates has also been found to help diminish the ohmic losses for these structures by reducing the current flow inside the metal. In addition, for CPW, the even and odd modes have been individually resolved in the time domain through the use of the electro-optic sampling technique, which can measure electric fields within either slot of the CPW. The attenuation and dispersion characteristics of CPS and CPW on a dielectric

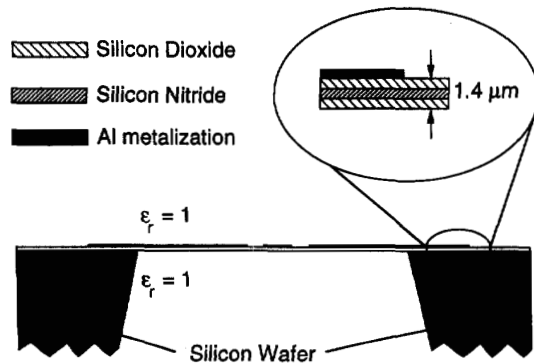


Fig. 1. Cross-sectional view of ultra-low-distortion coplanar waveguide with a 1.4- $\mu\text{m}$ -thick substrate of silicon dioxide and silicon nitride. The waveguide had a center strip width of 40  $\mu\text{m}$  and spacings of 25  $\mu\text{m}$ .

membrane, with their relatively flat behavior over a 1-THz bandwidth, suggest that these structures should be appropriate for circuit applications in the submillimeter-wave regime.

## II. SAMPLE STRUCTURE AND PREPARATION

Three different substrates, including GaAs, fused silica, and a composite dielectric membrane, have been used to support CPS and CPW lines in this experiment. The GaAs substrate was a semi-insulating wafer with a 1- $\mu\text{m}$ -thick low-temperature-grown GaAs (LT-GaAs) epilayer [7]. This served as a reference substrate for the transmission lines in order to highlight the degree of improvement that could be achieved by using the other low permittivity substrates. The second substrate employed was fused silica, which has uniform permittivity ( $\epsilon_r = 3.9$ ) and negligible dielectric loss between 300 GHz and 2 THz, as measured by an ultra-broadband time-domain spectroscopy technique [8]. The final substrate was a 1.4- $\mu\text{m}$ -thick dielectric membrane in a trilayer  $\text{SiO}_2/\text{Si}_3\text{N}_4/\text{SiO}_2$  configuration, with constituent thicknesses of 7000, 3000, and 4000 Å, respectively [9]. The base  $\text{SiO}_2$  layer was formed by thermal oxidation on a silicon wafer, followed by  $\text{Si}_3\text{N}_4/\text{SiO}_2$  low-pressure chemical vapor deposition. A section of the silicon substrate 3 mm  $\times$  10 mm was then removed by EDP (ethylene diamine pyrocatechol) etchant solution, leaving a free-standing dielectric membrane structure as shown in Fig. 1. This membrane, despite being very thin, has proven to be quite robust. Subsequent fabrication processing (including wafer cleaning, lithography, and deposition of metal lines) and electrical measurements were performed in a straightforward manner. CPS with 20  $\mu\text{m}$  strip widths and 20  $\mu\text{m}$  separation were patterned on all three substrates. The CPW lines, which were defined only on the GaAs and membrane substrates, had a center conductor width of 40  $\mu\text{m}$  and slot widths of 25  $\mu\text{m}$ . Due to the broadband nature of the experiment, all line dimensions above were chosen to avoid excessive radiation loss at high frequencies while holding the ohmic loss at low frequencies to a reasonable value.

A short-duration broadband electrical pulse, which was used as a test signal, was easily generated and launched *in situ* onto the transmission lines on the GaAs by using the substrate as a photoconductive pulse generator. The switch gap for the dc-biased coplanar lines, which was closed by laser irradiation,

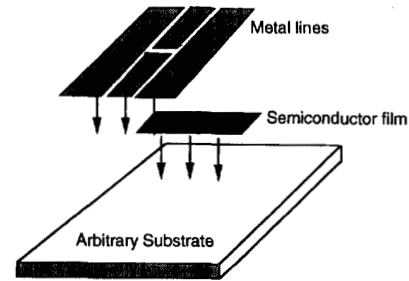


Fig. 2. Sample preparation procedure: an LT-GaAs epilayer lifted-off its native substrate by etching is grafted to a new substrate using a Van der Waals force bond. After forming the bond, standard lithography is used to print the metal pattern so that the switch gap covers the photoconductor.

was simply the slot between the two lines of the CPS or one of the slots in the CPW, although a gap interrupting the center line of the CPW was also used in certain tests. A 1- $\mu\text{m}$ -thick epitaxial layer grown on the GaAs substrate at the greatly reduced temperature of 200°C was utilized in order to provide a semi-insulating material with a carrier lifetime of less than 1 ps [7]. However, because both the membrane and the fused silica are very good insulators ( $\rho > 10^{14}$   $\Omega\text{-cm}$ ), the provision for optoelectronic device fabrication and signal generation that was inherent for the semiconductor wafer is not present in these other samples. However, this constraint was alleviated through the grafting of high-speed photoconductors onto the nonsemiconductor substrates by a Van der Waals bonding technique. Schottky photodiodes [10], HEMT-amplifier circuits [11], and laser diodes [12] have all been successfully lifted off and then Van der Waals bonded to different substrates. In this paper, in order to characterize the signal propagation on different substrates, 1- $\mu\text{m}$ -thick LT-GaAs thin films are isolated from their native substrates by chemical etching and then grafted to both silica and membrane substrates as *in situ* test-signal generators.

The procedure followed for this epitaxial lift off and grafting is a modified version of a technique outlined in [13], in which it is contended that the Van der Waals force is responsible for the moderate adhesion of the epitaxial film to a substrate. In the final bonding stage, we have found that thermal baking rather than pressure is most effective in forming the Van der Waals bond. Since the wax which is used to support the isolated film is soft at a higher temperature, it can serve as a good air-tight seal for the thin film and the substrate. Therefore, any space between the thin film and substrate left behind when the water diffuses out will remain in vacuum before being squeezed away by the atmospheric pressure. This thermal-baking method proves to be much better than that of placing a heavy block over the wax in terms of yield and processing time. For the results discussed here, the yield is very high and the time required to form the bond was less than an hour. Furthermore, the resulting LT-GaAs/low-permittivity substrate combination can withstand most standard low-temperature semiconductor processing steps. After forming the bond, standard lithography has been used to print the 1.4- $\mu\text{m}$ -thick aluminum metal line on the substrate. The process and the resulting test structure are shown in Fig. 2.

The resulting grafted LT-GaAs photoconductor has the same lifetime, mobility, and resistivity properties as it possessed before the lift-off procedure, and thus it produced nearly identical input signals for the three transmission lines.

### III. EXPERIMENTAL RESULTS

The laser used for the optoelectronic signal generation and measurement was a colliding pulse mode-locked dye laser with 80-fs pulse width and 100-MHz repetition rate. When the laser light was focused onto the photoconductive switch defined by the epitaxial LT-GaAs between the biased metal lines of the CPS or CPW, a short electrical transient was generated with full width half maximum (FWHM) as short as 0.8 ps. The fast onset of the pulse occurs as the energy from the short laser pulse is deposited onto the photoconductor, which then becomes less resistive, while the rapid fall time results from the ultrafast carrier lifetime of the LT-GaAs. The 3-dB bandwidth of the pulse is around 600 GHz, while there is measurable frequency content out to more than 1 THz.

Subpicosecond-duration voltage signals may readily be resolved using an electro-optic sampling probe, which consists of a tiny crystal of LiTaO<sub>3</sub> that is dipped into fringing electric fields above the transmission lines in order to sense the voltage present [14]. In this measurement technique, as the 80-fs laser pulses pass through the crystal, their intensity is modulated to a degree which is determined by the amplitude and phase of the microwave electric field present in the crystal during this 80-fs window. However, attaining consistent amplitude measurements is quite difficult because the electric field coupling between the probe and transmission line is very sensitive to the relative position of the probe. Since the low-frequency signals on the transmission line cannot couple into the probe as well as the high-frequency ones, the uncertainty in low-frequency data are typically larger than that at high frequencies. Therefore, great care has been taken during the measurements described herein to minimize the alignment error due to the probe movement. By comparing twenty data sets for each pulse measured, the error in the amplitude has been kept to around 10%, while the error in the pulse width is less than 100 fs.

Measurements in the time-domain have allowed a qualitative comparison of the different CPS and CPW lines through monitoring of the distortion of subpicosecond pulses as they propagated over various distances (Fig. 3). For the CPS-on-membrane, after 4 mm propagation, the waveform shows little of the pulse broadening and amplitude degradation normally associated with high-frequency transmission-line losses. Also absent are the increase in the rise time or the onset of trailing oscillations which are characteristic of modal dispersion and indicate that the higher frequency components in the pulse travel slower than the lower frequency components. Only a decrease in amplitude of less than 15%, which likely arose from skin-effect losses, was obvious, although the pulse width did increase slightly from 0.77 ps to 0.83 ps. For the CPS on fused silica, after 2 mm of propagation, the amplitude decreased to 75% of the input, while the pulse broadened to 1.2 ps. Some modal dispersion effects were also observed from the slower rising edge and faster trailing edge. However,

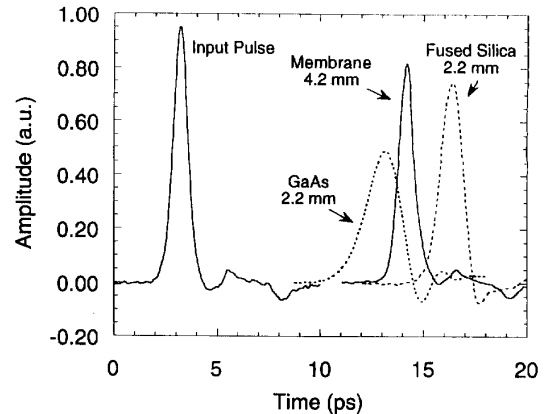


Fig. 3. Time domain waveforms for CPS on different substrates after various distances of propagation. The time delay for the pulses on the different substrates has been changed so that they all fit within the same time window.

for the signal on the GaAs substrate, after only 2 mm of propagation, the amplitude had already dropped to only 50% of the input value, and the pulse width broadened to 2.1 ps. Severe dispersion is also observed from the ringing in the tail. The 3-dB frequencies of the pulses after 3 mm propagation are 560, 375, and 180 GHz, for the membrane, fused silica, and GaAs substrates, respectively. For the CPW on the membrane, the improvement in waveform propagation over the CPW on GaAs is even greater. After 4-mm propagation, CPW on membrane still has over 80% of the input pulse amplitude. In contrast, the CPW on GaAs has lost over 70% of the input amplitude and the pulse width has stretched to 2.7 ps.

The time-domain data were also transformed to the frequency domain through the use of a fast Fourier transform routine so that a more quantitative analysis could be performed for these structures. By comparing frequency-domain data for pulses at two different propagation distances for all the transmission lines, the propagation factors have been determined for each. The attenuation coefficient and phase velocity were calculated over a wide range of frequency, extending to 1000 GHz for CPS on membrane. The resulting attenuation coefficient is shown in Fig. 4(a). The data for CPS on GaAs and CPS on fused silica are limited because the attenuation is large enough at the highest frequencies that there is not enough signal available to provide a suitable signal-to-noise ratio. Confirming the time-domain data, the CPS on membrane shows superior performance in the frequency range covered in the FFT. Virtually no radiation loss is observed in the 1-THz measurement band (where the attenuation would be proportional to  $f^n$ , where  $2 < n < 3$  [18]). Furthermore, the skin effect loss for the membrane CPS at 1000 GHz is comparable to that of the GaAs CPS at 150 GHz. The reason for such small skin-effect loss is the increase in impedance that occurs when the substrate permittivity is lowered. A higher impedance leads to a higher electric-to-magnetic field ratio, and thus more energy is stored in the electric field rather than the magnetic field for a pulse of the same energy content. Since

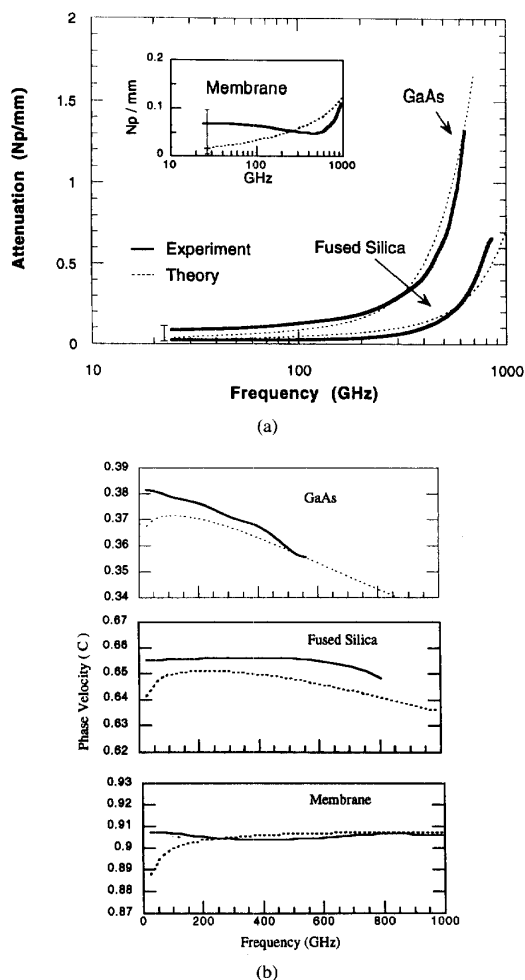


Fig. 4. (a) Experimental and theoretical attenuation coefficient of CPS on different substrates. (b) Phase velocity of CPS on different substrates. Solid lines are the experimental results. Dotted lines are from the theoretical simulation.

the current flow in the metal is proportional to the magnetic field surrounding the transmission line, the smaller magnetic-to-electric field ratio means less current flow in the metal and thus lower skin effect loss. The impedance for the CPS on the membrane is about  $240 \Omega$ , which is 2.4 times larger than that of the CPS on the GaAs substrate. Therefore, the skin-effect loss for CPS on membrane would be only 42% of that for the CPS on the GaAs substrate. This reduction in skin-effect loss is quite significant since this loss mechanism dominates for the membrane line.

For the CPS on fused silica, the attenuation is not dominated by the radiation loss until the frequency exceeds 350 GHz. While offering moderate bandwidth, the fused silica substrate provides a rigid support for the transmission line and any potential circuit components. This rigidity would be particularly important for a probe head used in an on-wafer microwave testing system, where a strong contact between the probe and circuit is needed. For the CPS on GaAs, the attenuation is en-

tirely dominated by radiation for frequencies above 200 GHz. This huge radiation loss makes it very difficult to operate such a coplanar line at high frequency.

The frequency-dependent phase velocity for the three CPS lines is shown in Fig. 4(b). For the CPS on membrane, a phase velocity of approximately 90% of the speed of light (which is virtually frequency-independent over a 1 THz band) has been found. Because of this low dispersion, signals can propagate with high fidelity. For the CPS on the fused silica substrate, the dispersion is small for frequencies below 500 GHz. Above that, with the electric field tending to concentrate in the higher-permittivity substrate, the phase velocity decreased. For CPS on GaAs, the phase velocity is already frequency-dependent for frequencies as low as 100 GHz. Thus, though the loss may be acceptable for signal bandwidth below 100 GHz, the dispersion can still create problems for high-speed digital signal propagation where low dispersion would be needed.

It should be noted that the rising edge of the pulse measured very close to the photoconductive switch on the membrane substrate is shorter than those switch outputs on the higher permittivity substrates. These rise times for the membrane, fused silica, and GaAs substrates are 0.72, 0.8, and 0.9 ps, respectively. These differences are due to the reduction in the parasitic capacitance associated with the substrate material. For digital circuits or fast-switching devices, low-permittivity substrates will result in less charging time and a faster slew rate. This is another potential advantage to circuit applications employing the substrates with a lower permittivity.

Another way to consider the superior waveguide performance of the CPS and CPW on these low-permittivity substrates is from a wavelength point of view. As the waveguide utilizes lower permittivity substrates, the phase velocity increases, along with the wavelength of the guided wave. As long as the wavelength is much larger in comparison to the size of the waveguide, the wave on the transmission line is quasi-TEM-like, leading to less dispersion and radiation. One way to make the wavelength much larger than the size of the waveguide is to reduce the size of the waveguide itself, i.e., to reduce the size of the metal line. Although this method helps in reducing the radiation loss at high frequency, it severely increases the metal skin effect loss for all frequencies. However, if the substrate permittivity is made to be very close to that of air, not only is the radiation loss eliminated, but the metal ohmic loss can also be reduced by increasing the metal line size. Therefore, the latter approach would yield a superior overall performance. One problem arises when considering the impedance, since it would be more difficult for the CPS lines on a low permittivity substrate to obtain  $R_c = 50 \Omega$ . However, for high-frequency operation, where low loss and low dispersion are the primary considerations, shifting the design to higher impedance would be more practical than keeping the line at an impedance where the loss and dispersion is unacceptable. Still, for CPW on membrane or fused silica substrates, it is still possible to attain a  $50\text{-}\Omega$  line impedance, although some performance degradation will result. Despite this, CPW on membrane is unquestionably superior to a CPW on GaAs with the same impedance.

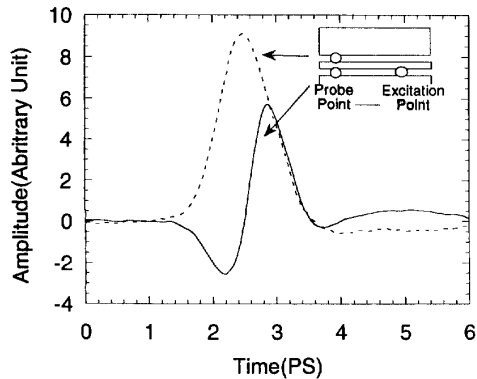


Fig. 5. Waveforms measured by electro-optic sampling in the two slots of the CPW.

The electro-optic sampling probe, which is used to sense the electric field of a signal, is also flexible enough that it can measure the fields within the slots between either of the ground lines and the center conductor of CPW. By exciting the pulsed test signals asymmetrically, through a shunt photoconductive switch which can be defined at any location along the CPW within either of the slots, we have generated both even and odd modes on the CPW and measured their waveforms in each slot at the same propagation distance of 4 mm. The direction of the electric field of the two modes was the same across one slot and opposite across the other, so that the even and odd modes could be individually resolved. The observation of these modes has been clarified by adding or subtracting the waveforms from the opposing slots. This method provides a more straightforward way than the frequency-domain measurement to investigate the propagation of the different modes on CPW. Fig. 5 shows the actual measured waveforms from opposite sides of the CPW on the membrane substrate. From the polarity difference in the measurement from one of the slots, the signal is identified as a linear superposition of the even and odd modes. The field from the even and odd modes is in the same direction in the other slot, yielding a superposition that is unipolar. When these two waveforms from the opposing slots are simply added and subtracted, we are left with the result in Fig. 6(a). This shows that the CPW on the membrane has extremely good propagation characteristics for the even mode as compared with that for the CPW on GaAs [Fig. 6(b)], which is very lossy and dispersive. In addition, the group velocity of the odd and even modes was determined to differ by 5% for the membrane CPW and 20% for the GaAs CPW.

The phase velocity of the even mode is expected to be larger than that of the odd mode because more electric field lines are in the air for the even mode. This, of course, lowers the effective permittivity for the even mode so that it is somewhat less than that of the odd mode. Indeed, from a determination of the group velocity (which can be measured directly in the time domain), the even mode, in fact, propagates at a slower speed. This also indicates that the even mode should suffer a larger dispersion than the odd mode. That this is true can be observed

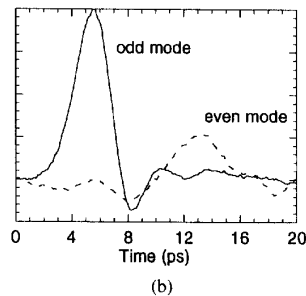
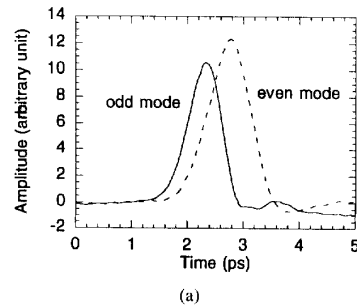


Fig. 6. Experimental observation of the separation of odd and even modes in a subpicosecond transient propagating on coplanar waveguide on (a) a membrane and (b) GaAs after 4 mm propagation.

by inspecting the pulse rise time of the signal representing the even mode, which is longer than that of the odd mode.

The excitation of even modes is an important problem in circuit design, where the even mode can be generated because of the asymmetry of the structure or the asymmetry of the excitation. The effect of even mode excitation on coplanar waveguide performance has been studied extensively by numerous authors [15], [16], and a limited number of solutions have been suggested through the use of air-bridges or appropriate circuit layout. However, the CPW on membrane, because of its inherently longer wavelength and a much smaller difference in propagation speed for the two modes, would be less sensitive to circuit asymmetries of comparable size to those typically found on GaAs substrates.

#### IV. THEORY

Semi-empirical models for the attenuation and dispersion of CPS and CPW are well established and have been found to agree quite well with experiments [17], [18]. For simplicity, only the equations for CPS are shown here, although similar equations apply to CPW through adjustment of the coefficients. Basically, the transmission line is modeled as an  $R, L, G, C$  lumped-element equivalent circuit. Due to the low-loss nature of the substrates considered here, the conductance term  $G$  is ignored. The propagation constant in terms of the equivalent circuit is

$$\gamma = \alpha(f) + j\beta(f) = j\omega\sqrt{LC} \left[ 1 - \frac{jR}{2\omega L} \right] \quad (1)$$

where  $\alpha(f)$  is the attenuation coefficient and  $\beta(f)$  is the phase factor at frequency  $f$ . Since the pulse can be decomposed by

the Fourier transform, each Fourier component of the pulse at frequency  $f$  after  $z$  propagation distance can be written as

$$A(f, z) = A(f, 0) \exp[(-\alpha(f) + j\beta(f))z]. \quad (2)$$

After obtaining all the Fourier components of the pulse after the propagation over distance  $z$  by the above relations, the time-domain waveform at  $z$  can be calculated using the inverse Fourier transform.

The capacitance term  $C$  depends strongly on effects due to the substrate. As pointed out in the previous section, the high-frequency components in the pulse tend to travel slower than the low-frequency ones, due to the amount of field constrained in the substrate at different frequencies. A semi-empirical formula for the effective permittivity  $\epsilon_{\text{eff}}(f)$  in [19] is incorporated to include this effect, and the capacitance is then given as

$$C = \epsilon_{\text{eff}}(f)\epsilon_0[K'(k)/K(k)] \quad (3)$$

where  $k = s/(s + 2w)$ ,  $\epsilon_0$  is the permittivity of vacuum,  $K$  is the complete elliptic integral of the first kind, and  $K' = K[(1 - k^2)^{1/2}]$ . For the membrane, the experimental phase velocity is used to determine the  $\epsilon_r$  in the expression of  $\epsilon_{\text{eff}}(f)$  [19]. However, this  $\epsilon_r$  can also be theoretically estimated to first order from the equations in [20]. The inductance term  $L$  depends on the magnetic field, which is frequency independent and is given as

$$L = \mu_0[K(k)/K'(k)]. \quad (4)$$

The resistance term,  $R$  is related to the surface impedance of the metal and the geometric dimensions of the transmission line. It is given as

$$R = Z_S g \quad (5)$$

where  $g$  is a geometric factor given in [21], and  $Z_S$  is the surface impedance of the metal line

$$Z_S = (1 + j)/(\delta\sigma) \coth\{(1 + j)t/\delta\} \quad (6)$$

where  $\delta$  is the metal skin depth,  $t$  is the thickness of the metal, and  $\sigma$  is its conductivity. Since the surface impedance has both real and imaginary parts, the term  $R$  affects both the attenuation and dispersion.

As mentioned in the introduction, the high-frequency components on the transmission line radiate energy into the substrate. For this radiation loss, the resistance term alone is not enough to describe the high-frequency behavior. Therefore, a radiation-loss term is incorporated to describe the loss at high frequency [18].

$$\alpha_{\text{rad}}(f) = \pi^5 \frac{(3 - \sqrt{8})}{2} \sqrt{\frac{\epsilon_{\text{eff}}(f)}{\epsilon_r}} \left(1 - \frac{\epsilon_{\text{eff}}(f)}{\epsilon_r}\right)^2 \cdot \frac{(s + 2w)^2}{c^3 K'(k) K(k)} f^3 \quad (7)$$

where  $s$  is the CPS separation,  $w$  is the strip width, and  $c$  is the speed of light. Equation (7) is valid only when  $\lambda \gg (s + 2w)$ , otherwise the radiation loss will decrease with increasing

frequency in a nonphysical fashion. After taking into account the radiation loss, the total loss  $\alpha(f)$  is

$$\alpha(f) = \alpha_{\text{rad}}(f) + \left[ \frac{\text{Re}(R)}{2Z_0} \right] \quad (8)$$

where  $Z_0$  is the characteristic impedance of the transmission line. For the dispersion, the  $\beta(f)$  is

$$\beta(f) = \left[ \frac{\omega\sqrt{\epsilon_{\text{eff}}}}{C} + \frac{\text{Im}(R)}{2Z_0} \right]. \quad (9)$$

The simulated attenuation coefficient and phase velocity are shown in Fig. 4(a) and (b). Even with a simple lumped-element equivalent circuit model, a good agreement with the experimental observation has been obtained. This comparison also verified the validity of these equations for the low-permittivity substrate. The surface-wave loss is not considered here because of the nature of the short-duration broadband testing signal used in the experiment. Since the signal roundtrip time across the substrate (GaAs, fused-silica) is greater than the measurement time-window, the loss is dominated by the radiative term only. For the line on the membrane substrate, since the cutoff frequency for surface waves are very high, the surface-wave attenuation is not considered either.

The discrepancy between theory and experiment in the phase velocity at low frequency is due to a finite time-domain truncation error in the data reduction. In order to characterize the transmission line at low frequency, a very long time window is needed. However, in order to keep unwanted noise and reflections from being processed by the Fourier transform, a finite time window is selected from the time-domain measurement. The effect of truncation error can be observed by artificially cutting the time-domain waveform generated by the equations above and then computing the Fourier transform again to calculate the phase velocity. The result shows that there is no difference at high frequencies, while at low frequencies the phase velocity increases, as is also observed in the experimental frequency-domain data.

## V. SUPPRESSION OF PULSE TAIL ON MEMBRANE COPLANAR LINES

As pointed out by several authors [5], [22], the long dc-like tail which is typically observed in the time domain for transmission lines having a thin metallization arises principally from low-frequency metal loss, where the skin depth is larger than the metal thickness. This phenomenon can be verified by varying the metal thickness, so that as the metal becomes thinner, the amplitude of the shoulder and the length of the tail increase. For applications like time-domain device characterization, the resistive tail will result in the inaccuracy of low-frequency data because of the time-domain truncation error as discussed above. For digital-signal propagation, this effect will cause the signal to ride on a dc background, which for a thin metallization and long propagation distance, may be higher than the low-logic level. To eliminate the tail, the metallization should be as thick as possible so that the metal thickness is larger than the metal skin depth, even at low

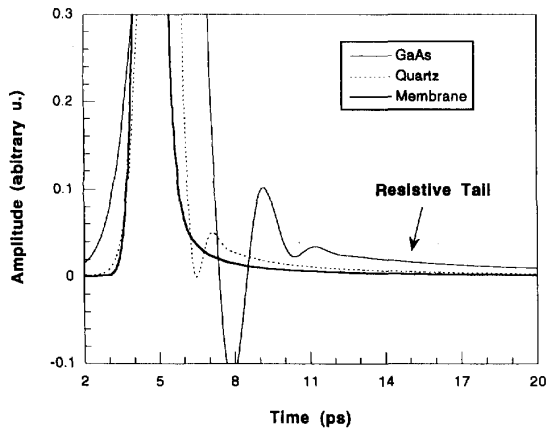


Fig. 7. Simulation of resistive tail of CPS on three different substrates after 4 mm propagation with a 1 ps Gaussian input pulse.

frequency. However, to reduce the length of the resistive tail to a few picoseconds, several micrometers of metal are required, which is not practical for integrated circuits. However, by changing the substrate to one with lower permittivity, the resistive tail is suppressed very well even with a moderate metal thickness. Due to the amplitude uncertainties associated with electro-optic sampling at low frequencies, we have studied the resistive tail using the equations from the previous section. Fig. 7 shows the simulation results for a 1-ps FWHM Gaussian pulse after 4 mm propagation on a CPS on different substrates (metal thickness is  $1.4 \mu\text{m}$ ). Even with this thickness, the tail for the pulses on the GaAs CPS lasts for several tens of picoseconds. In contrast, for the pulse on the membrane CPS, not only is the shoulder amplitude smaller, but the tail also disappears in only a few picoseconds.

## VI. CONCLUSION

The propagation of short pulses on CPS and CPW transmission lines on membrane, fused silica, and GaAs substrates has been characterized in both time and frequency domains. Epitaxial lift-off and Van der Waals bonding is used to integrate LT-GaAs photoconductive switches onto different substrates for use as test-signal-generator sites. This technique may also be used to integrate active and passive devices onto the membranes, allowing development of a high-speed integrated-circuit family. For the CPS and CPW on the membrane substrate, a bandwidth greater than 1 THz and very low dispersion have been demonstrated. The near-TEM wave propagation on the membrane also makes it possible to extend passive circuit design at low frequency directly to high frequency. Moreover, since the wavelength is longer when the low permittivity substrate is used, the signal is less sensitive to waveguide discontinuities such as bends. For the fused silica CPS, improvement can be made to its propagation characteristics by adding a matching superstrate. The standard passivation layer in semiconductor processing is silicon dioxide, which has approximately the same permittivity

as fused silica. Therefore, when the passivation is put on the substrate to protect the device, a superstrate is added to the waveguide at the same time. Raising the line impedance has been shown to be advantageous not only in reducing the skin effect loss at high frequency, but also for diminishing the tail generated by low-frequency metal loss. For ultra-high frequency applications where low loss and low dispersion are needed, metal lines on low-permittivity substrates are likely to perform considerably better than even superconducting lines.

## ACKNOWLEDGMENT

The authors thank F. Smith of the Massachusetts Institute of Technology, Lincoln Laboratory for providing low-temperature grown GaAs layers.

## REFERENCES

- [1] S. Y. Chou and M. Y. Liu, "Nanoscale tera-hertz metal-semiconductor-metal photodetector," *IEEE J. Quantum Electron.*, vol. 28, pp. 2358–2368, 1992.
- [2] W. C. B. Peatman, P. A. D. Wood, D. Porterfield, and T. W. Crowe, "Quarter-micrometer GaAs Schottky barrier diode with high video responsivity at 118  $\mu\text{m}$ ," *Appl. Phys. Lett.*, vol. 61, pp. 294–296, 1992.
- [3] D. Grischkowsky, I. N. Duling, III, J. C. Chen, and C.-C. Chi, "Electromagnetic shock waves from transmission lines," *Phys. Rev. Lett.*, vol. 59, pp. 1663–1666, 1987.
- [4] J. Nees, S. Williamson, and G. Mourou, "100 GHz traveling-wave electro-optic phase modulator," *Appl. Phys. Lett.*, vol. 54, pp. 1962–1964, May 1989.
- [5] U. D. Keil, *et al.*, "High-speed coplanar transmission lines," *IEEE J. Quantum Electron.*, vol. 28, pp. 2333–2342, 1992.
- [6] W. H. Knox, "Quantum well for femtosecond optoelectronics application," *Appl. Phys.*, vol. A53, pp. 503–513, 1991.
- [7] S. Gupta, *et al.*, "Subpicosecond carrier lifetime in GaAs grown by molecular beam epitaxy at very low temperatures," *Appl. Phys. Lett.*, vol. 59, pp. 3276–3278, Dec. 1991.
- [8] J. M. Chwalek, J. F. Whitaker, and G. A. Mourou, "Low-temperature epitaxially-grown GaAs as a high-speed photoconductor for terahertz spectroscopy," in T. C. L. G. Sollner and J. Shah, Eds., *OAS Proceedings on a Picosecond Electronics and Optoelectronics*. Washington, D.C.: Optical Society of America, 1991, pp. 15–19.
- [9] N. I. Dib, W. P. Harokopos, L. P. B. Katehi, C. C. Ling, and G. M. Rebeiz, "Study of a novel planar transmission line," *IEEE MTT-S Int. Symp. Dig.*, 1991.
- [10] F. Kobayashi and Y. Sekiguchi, "GaAs Schottky photodiode fabricated on glass substrate using epitaxial lift-off technique," *Jpn. J. Appl. Phys.*, pt. 2, vol. 31, pp. 850–852, 1992.
- [11] P. G. Young, R. R. Romanofsky, S. A. Alterovitz, R. A. Mena, and E. D. Smith, "A 10-GHz amplifier using an epitaxial lift-off pseudomorphic HEMT device," *IEEE Microwave Guided Wave Lett.*, vol. 3, pp. 107–109, 1993.
- [12] W. K. Chan, A. Yan, and T. J. Gmitter, "Grafted semiconductor optoelectronics," *IEEE J. Quantum Electron.*, vol. 27, no. 3, pp. 717–725, 1991.
- [13] E. Yablonovitch, D. D. Hwang, T. J. Gmitter, L. T. Flores, and J. P. Harbison, "Van der Waals bonding of GaAs epitaxial lift-off films onto arbitrary substrates," *Appl. Phys. Lett.*, vol. 56, pp. 2419–2421, 1989.
- [14] J. A. Valdmanis and G. A. Mourou, "Subpicosecond electrooptic sampling: Principles and applications," *IEEE J. Quantum Electron.*, vol. 22, pp. 69–78, 1986.
- [15] N. I. Dib, M. Gupta, G. E. Pouchak, and L. P. B. Katehi, "Characterization of asymmetric coplanar waveguide discontinuities," *IEEE Trans. Microwave Theory Tech.*, vol. 41, pp. 1549–1558, Sept. 1993.
- [16] M. Tsuji, H. Shigesawa, and A. A. Oliner, "New interesting leakage behavior on coplanar waveguides of finite and infinite widths," *IEEE Trans. Microwave Theory Tech.*, vol. 39, pp. 2130–2137, 1991.
- [17] J. F. Whitaker, R. Sobolewski, D. R. Dykaar, T. Y. Hsiang, and G. A. Mourou, "A propagation model for ultrafast signals on superconducting dispersive striplines," *IEEE Trans. Microwave Theory Tech.*, vol. 36, pp. 277–285, 1988.

- [18] M. Y. Frankel, S. Gupta, J. A. Valdmanis, and G. A. Mourou, "Terahertz attenuation and dispersion characteristics of coplanar transmission lines," *IEEE Trans. Microwave Theory Tech.*, vol. 39, pp. 910-916, 1991.
- [19] G. Hasnain, A. Dienes, J. R. Whinnery, "Dispersion of picosecond pulses in coplanar transmission line," *IEEE Trans. Microwave Theory Tech.*, vol. 34, pp. 738-741, 1986.
- [20] W. H. Knox, *et al.*, "Femtosecond excitonic optoelectronics," *IEEE J. Quantum Electronics*, vol. 25, pp. 2586-2595, 1989.
- [21] W. J. Gallagher, *et al.*, "Subpicosecond optoelectronic study of resistive and superconductive transmission lines," *Appl. Phys. Lett.*, vol. 38, pp. 277-279, 1988.
- [22] L. P. Golob, S. L. Huang, and C. H. Lee, "Picosecond photoconductive switches designed for on-wafer characterization of high frequency interconnects," In: *1993 IEEE MTT-S International Symposium Digest*, p. 1395.



**Heng-Ju Cheng** received the B.S. and M.S. degrees from National Chao Tung University, Taiwan, in 1985 and 1987, respectively. He is currently working towards the Ph.D. degree at the University of Michigan, Ann Arbor.

Upon completion of military service, he joined the Industrial Technology Research Institute, Taiwan, between 1989 to 1990 as a Device Engineer for developing charge couple device. His research interests include high speed device characterization, high speed photodetectors, and ultrafast optically

based measurement techniques in the submillimeter wave regime.



**John F. Whitaker** (S'84-M'88) received the B.Sc. degree in physics from Bucknell University, Lewisburg, PA, in 1981, and the M.Sc. and Ph.D. degrees from the University of Rochester, Rochester, NY, in 1983 and 1988, respectively.

In 1989, he accepted a position as a Research Scientist in the Ultrafast Science Laboratory within the Department of Electrical Engineering and Computer Science at the University of Michigan, Ann Arbor. He is also currently the coordinator for the Ultrafast Technology area within the National Science

Foundation Science and Technology Center for Ultrafast Optical Science. His research interests include the development of ultrahigh temporal response, optically-based measurement systems and their application to measurements of the response of semiconductors, superconductors, dielectrics, transmission lines, devices, and circuits on picosecond and subpicosecond time scales. He has authored or coauthored more than 50 papers and has presented nine invited talks at major conferences and symposia.



**Thomas M. Weller** was born in Battle Creek, MI, in November, 1965. He received the B.S.E.E. and M.S.E.E. degrees from the University of Michigan, Ann Arbor, in 1988 and 1991, respectively. He is currently pursuing the Ph.D. degree in electrical engineering at the same university.

His present research involves micromachining applications for microwave circuits and numerical modeling in electromagnetics.

**Linda P. B. Katehi** (S'81-M'84-SM'89), for a biography, see page 83 of the January issue of this TRANSACTIONS.